第 35 卷第 1 期
2019 年 1 月

无 机 化 学 学 报
CHINESE JOURNAL OF INORGANIC CHEMISTRY

Vol.35 No.1
174-182

发光的异核稀土配合物装饰氧化石墨烯片

李运涛 邱 硕* 杜 滕 魏 巍 韩振斌 阮方毅 曹丽慧
(陕西科技大学,陕西省轻化工助剂重点实验室,西安 710021)

摘要：采用非共价键的方法制备一种新型的高荧光性能氧化石墨烯–异核稀土杂化材料。利用苯甲酸(BA)和菲咯啉(Phen)与 Sm^{3+}和 Gd^{3+}配位,并作用在氧化石墨烯片(GOSs)表面,制备了一种异核稀土配合物。所制备的产物通过傅里叶变换红外光谱、X射线衍射、扫描电子显微镜、荧光光谱仪、荧光寿命和热重分析来表征。该杂化材料具有强发光强度、长的寿命和良好的热稳定性。此外,Gd^{3+}对材料具有很强的敏化作用,同时 Gd^{3+}在提高发光强度方面起着重要作用。氧化石墨烯的存在不会淬灭杂化材料的荧光性能。此外,还研究了具有不同物质的量之比的 Sm^{3+}和 Gd^{3+}的荧光特性。

关键词：氧化石墨烯；钐；稀土；发光
中图分类号：O614.33 **文献标识码**：A **文章编号**：1001-4861(2019)01-0174-09
DOI:10.11862/CJIC.2019.016

Decoration of Graphene Oxide Sheets with Luminescent Heteronuclear Rare-Earth Complexes

LI Yun-Tao QIU Shuo* DU Teng WEI Wei HAN Zhen-Bing RUAN Fang-Yi CAO Li-Hui
(*Shaanxi Key Laboratory of Chemical Additives for Industry , Shaanxi University of Science and Technology, Xi'an* 710021, *China*)

Abstract: A novel high luminescent performance of graphene oxide-rare earth hybrid material was prepared using a noncovalent approach. Herein, a heteronuclear rare earth complex were revealed in which the benzoic acid (BA) and 1,10-phenanthroline hydrate (Phen) coordinated with Sm^{3+} and Gd^{3+}, which was used to functionalize graphene oxide sheets (GOSs). The as-prepared products were characterized via Fourier-transform infrared spectroscopy, X-ray diffraction, scanning electron microscope, fluorescence spectrometer, decay lifetime and thermogravimetric analysis. The hybrid materials exhibited strong luminescence intensity, long lifetime and good thermal stability. Besides, Gd^{3+} ions had a strong sensitizing effect on materials and played a significant role in improving the luminescence intensity. The presence of GOSs did not quench the fluorescence performance of hybrid materials. Moreover, their fluorescence properties of Sm^{3+} and Gd^{3+} with different molar ratios were also studied.

Keywords: graphene oxide; samarium; rare earths; luminescence

0 Introduction

Graphene, a single layer of carbon atoms arranged in honeycomb structures, has attracted extensive attentions since the advent of free-standing graphene sheets in 2004[1]. The two-dimensional carbon nonmaterial, such as graphene have been widely explored recently to demonstrate its potential applications in biomedical study and by fabricating graphene based nano-scaled electronic, optoelectronic, photovoltaic and sensing devices[2-4]. The optical response of graphene can be described by the surface conductivity which is

收稿日期:2018-09-26。收修改稿日期:2018-11-13。
国家自然科学基金青年项目(No.21701106)资助。
*通信联系人。E-mail:roseofsnow@163.com

originated from the contributions of inter-band and intra-band transitions, related to the chemical potential or Fermi level[5-6]. Recently a weak and wide photoluminescence peak of graphene oxide has been reported[7]. In spite of massive investigation has been carried out to address the origin of the fluorescence, there is not a single and strong theory. In addition, it has been established that the sp^2 units have a vital role in the emission of the light but the π-π* transitions in the sp^2 units of aromatic sections are not the only reason[8-9].

Rare earth (RE) organic complexes not only show high luminous intensity but also high fluorescence quantum yield, they have been widely used in medical testing, drug analysis, environmental monitoring, security fields and other characteristics[10-13]. It is well known that fluorescence enhancement could be achieved through ligand sensitization, but using certain second lanthanide ions such as Gd^{3+} and La^{3+} could also increase the fluorescence properties [14-15]. Due to the unique properties of GOSs, RE complexes are deposited on the surface of GOSs may obtain high performance luminescent hybrid materials. However, when used in practice, fluorescence performance of GOSs hybrid materials is not as good as expected, the luminescences need to be enhanced, but conventional luminescent tags such as dye molecules have to face a challenge that GOSs have a fluorescence quenching effect[16]. Therefore, how to improve the fluorescence properties of hybrid materials becomes a meaningful thing. Recently there are some works of GOSs/RE has been prepared successfully. Cao and co-worker[17] reported GOSs functionalized with RE complexes using a non-covalent approach and GOSs hybrid materials can be easily exfoliated into single-layer sheets. Zhang and co-worker[18] synthesized a novel complex material Eu-modifed reduced GO (graphene oxide) by the simple stirring process through has been proposed. Wang and co-worker[19] reported a simple and effective method synthesized GOSs/Eu-acac-Phen (acac=acetylacetone) via non-covalently functionalized GOSs, the GOSs enhance the fluorescence lifetime of the complexes. Fan and co-worker[20] successfully synthesized luminescent Sm^{3+} complexes [$Sm(TTA)_3$ Phen] (TTA =2 -thenoyltrifluoroacetone) via covalent functionalization to surface-carboxylated graphene oxide (GO-COOH). Zhao and co-worker[21] successfully prepared graphene oxide/$Eu(TTA)_3$Phen complex hybrid materials via an innovation method, which had better stability. Zhang and co-worker[22] reported a novel graphene oxide-rare earth complex hybrid materials [Eu-TTA-PMA/GOSs] (PMA=pyromellitic acids) through non-covalent approach, the material also exhibits stronger luminescence intensity, long decay lifetime and better thermal stability. In this paper, the π-electron of the graphene oxide and the conjugated structure of the ligand are combined by the π-π stacking method of non-covalent bond. The carbon atoms in graphene oxide form a highly delocalized π electron by sp^2 hybridization. These π electrons can be combined with other materials having a large π conjugate structure through π-π interaction to achieve good dispersion of graphene oxide, that the non-covalent bond function method of graphene oxide is most commonly used in chemical applications.

In this work, we present a heteronuclear Sm^{3+} and Gd^{3+} RE complex (Sm-Gd)BA_3Phen via noncovalently functionalized GOSs based on BA as the main ligand, Phen as the ancillary ligand. Gd^{3+} ions obviously improved the fluorescence of hybrid material and played a significant role. Moreover, we synthesized the hybrid materials with bright red luminescence, and the characteristic fluorescence of Sm^{3+} is $^4G_{5/2}$-$^6H_{5/2}$, $^4G_{5/2}$-$^6H_{7/2}$, and $^4G_{5/2}$-$^6H_{9/2}$ transitioned at 563, 596 and 604, and 643 nm excited by UV light. The hybrid materials obtained the best luminescence property when $n_{Sm^{3+}}$:$n_{Gd^{3+}}$ was 5:5.

1 Experimental

1.1 Materials and instrumentation

Natural flake graphite was purchased from Sinopharm Chemical Reagent Co., Ltd. Samarium oxide (Sm_2O_3, 99.99%) were purchased from Sinopharm Chemical Reagent Co., Ltd. Benzoic acid were purchased from Tianjin Bai Shi Chemical Co., Ltd. 1,10-phenanthroline (Phen) were purchased from Tianjin Branch Miou Chemical Reagent Co., Ltd. All the reagents for the analysis are of pure and used without further purification.

Fourier Transform infrared spectroscopy (FT-IR) the United States Perkin Elmer 2000 Fourier transform infrared spectrometer (KBr tablet). Fluore-scence spectrometry (FS) was obtained by with Germany HORTBA Scientific Fluormax-4P Spectrofluorometer. The thermo-gravimetric analyzer (TAG) was performed Germany Netzsch PLT-400 type integrated thermal analyzer. X-ray diffraction (XRD) was obtained by the Shimadzu XRD-7000S/L type automatic X-ray diffractometer with a voltage of 40 kV and a current of 30 mA at a scanning rate of 8.0°·min^{-1}. The diffraction angle was conducted in a range of 4°~50° with Cu $K\alpha_1$ radiation (λ=0.154 06 nm). Scanning electron microscopy (SEM) was obtained by Japanese Hitachi Model S-4800. The secondary electron resolution was 1.0 nm (15 kV), the magnification was 8 000 and the acceleration voltage was 3.0 kV.

1.2 Preparation of pure (Sm-Gd)BA$_3$Phen complex

Graphene Oxide was prepared by modified Hummers methods[23-24]. Firstly, 1 mmol of samarium oxide (Sm_2O_3) was completely dissolved in 15 mL of concentrated hydrochloric acid, and slowly steamed in the water bath to remove excess acid. The 20 mL of 99%(*V*/*V*) absolute ethanol was added to obtain 0.05 mol·L^{-1} $SmCl_3$ ethanol solution. Then 1 mmol of gadolinium chloride ($GdCl_3$) was dissolved in 20 mL ethanol solution to prepare 0.05 mol·L^{-1} $GdCl_3$ ethanol solution. A certain amount of BA and Phen was weighted according to n_{SmCl_3}:n_{BA}:n_{Phen}=1:3:2, mixed in a three-necked flask and kept stirring. The $SmCl_3$ and $GdCl_3$ ethanol solution was added dropwise to the system and $n_{Sm^{3+}}$:$n_{Gd^{3+}}$ was 5:5. Then, the pH value was adjusted to 6~7 with 0.1 mol·L^{-1} NaOH aqueous solution. The mixture was heated and stirred for 5 h at 70 ℃. The white precipitate was obtained and placed for 24 h. Finally the mixture was filtered and washed with ethanol several times. The precipitate was dried at 60 ℃.

1.3 Synthesis of GOSs/(Sm-Gd)BA$_3$Phen complex hybrids

Firstly, 10 mg as-prepared GOSs were dispersed in 20 mL ethanol and vibrierened for 2 h. Secondly the obtained 0.05 mol·L^{-1} $SmCl_3$ ethanol solution and 0.05 mol·L^{-1} $GdCl_3$ ethanol solution were added to the solution of GOSs in ethanol to vibrieren for 0.5 h. After these treatments, 0.73 g (6 mmol) of BA and 0.72 g (4 mmol) of Phen were dissolved in 20 mL ethanol and dropped into the above suspension under the strong agitation. The pH value of solution was adjusted to 6~7 by 0.1 mol·L^{-1} NaOH aqueous solution. The mixture was heated and stirred for 5 h at 70 ℃. Finally, after being placed for 24 h, the product were washed with ethanol several times and dried at 60 ℃. Schematic illustration of the preparation of GOSs/(Sm-Gd)BA$_3$Phen complex hybrid is shown in Fig.1.

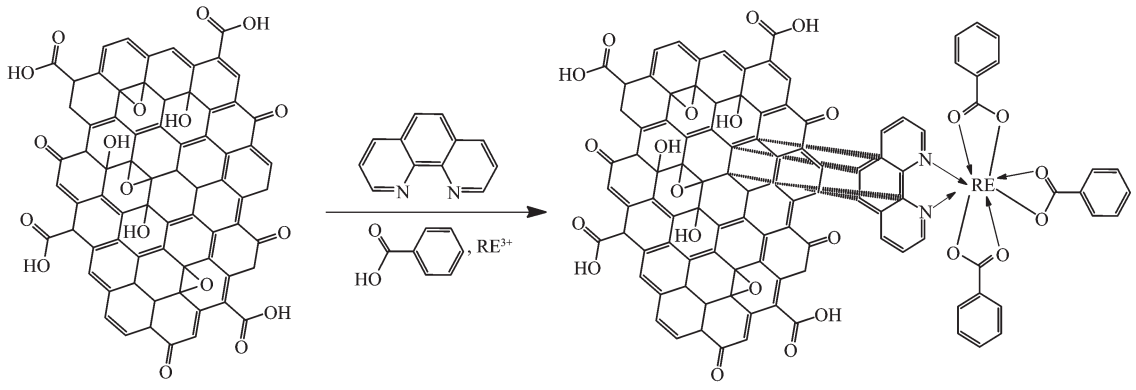

Fig.1 Schematic illustration of preparation of GOSs/(Sm-Gd)BA$_3$Phen complex hybrid (RE=Sm, Gd)

2 Results and discussion

2.1 FT-IR characterization

In order to provide a more detailed composition of the chemical bonds and the functional groups, GOSs, (Sm-Gd)BA$_3$Phen, GOSs/(Sm-Gd)BA$_3$Phen complex hybrid were characterized by FT-IR as shown in Fig.2 and the spectral region was 4 000~400 cm^{-1}. The

characteristic absorption peak of GOSs at 1 728 cm^{-1} was assigned to C=O stretching vibration, the peak of C=C was at 1 620 cm^{-1}, the peak of -OH deformation vibration was at 1 403 cm^{-1} and the peak of symmetric stretching vibration of epoxy bond was at 1 050 cm^{-1} indicating successful synthesis of GOSs[25]. The characteristic peak of BA are assigned to C=O (1 660 cm^{-1}) and C-O (1 281 cm^{-1}), and disappeared after (Sm-Gd)BA_3Phen complex was formed. The peak of -COO stretching vibration was at 1 410 cm^{-1}, which illustrated that the acid radical was involved in the coordination. The characteristic absorption peaks of Phen at 1 639 and 1 578 cm^{-1} correspond to C=C and C=N stretching vibrations[26], respectively, which were shifted to 1 613 and 1 573 cm^{-1}, indicating that N atoms had coordinated with RE ions. The peak of C-H bending vibration at 744 and 850 cm^{-1} were shifted to 731 and 846 cm^{-1}, which also indicated that N atoms had coordinated with RE ions. In addition, around 426 and 660 cm^{-1} correspond to Sm-O stret-ching vibration[27]. Fig.2 shows the peak at 1 519 cm^{-1} of GOSs/(Sm-Gd)BA_3Phen complex hybrid compared with (Sm-Gd)BA_3Phen complex was broaden. It may provide strong evidence for deprotonated -COOH coordinated to Sm^{3+} as $-COO^-$. This shows that RE ion is easy to carboxyl and carbonyl coordination.

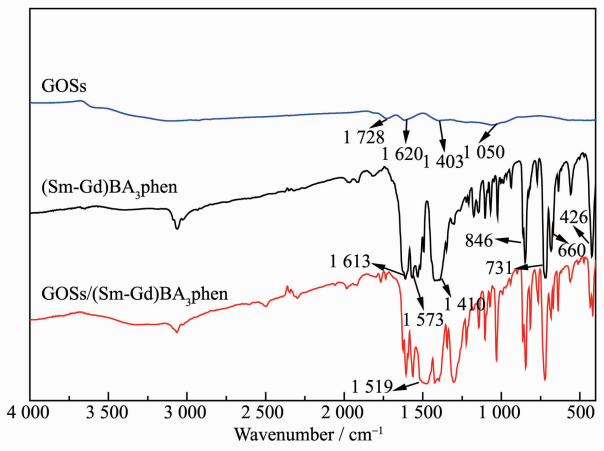

Fig.2　FT-IR spectra of GOSs, (Sm-Gd)BA_3Phen and GOSs/(Sm-Gd)BA_3Phen

2.2　XRD

X-ray diffraction was used to study the crystal structure of GOSs, (Sm-Gd)BA_3Phen complex and GOSs/(Sm-Gd)BA_3Phen complex hybrid (Fig.3). There is a sharp peak at 10.32° in Fig.3(a), which is the characteristic peak of GOSs[28]. The interlayer spacing of GOSs was 0.759 nm which is much larger than that of pristine graphite (about 0.337 nm) due to the presence of the oxygen-containing functional groups on the surfaces of the graphite sheet[29]. The XRD of (Sm-Gd)BA_3Phen complex in Fig.3(b) shows two diffraction peaks at 2θ=23.77° and 27.8°, which belong to the reflection of Phen and $SmCl_3$[30], respe-ctively. This means that Phen and $SmCl_3$ did not react completely during the complex formation. As shown in Fig.3(c) the reflection of GOSs disappeared after GOSs combined with Sm complex. This suggests that the interlayer structure of GOSs have been destroyed by (Sm-Gd)BA_3Phen complex[31-32]. The diffraction peaks of GOSs/(Sm-Gd)BA_3Phen complex hybrid at 2θ=12.57° and 8.6° appeared. Hence, the results illustrate the crystal structure of (Sm-Gd)BA_3Phen complex and GOSs disappeared and GOSs/(Sm-Gd)BA_3Phen complex hybrid formed a new crystal structure, which is different from both GOSs and (Sm-Gd)BA_3Phen complex[21].

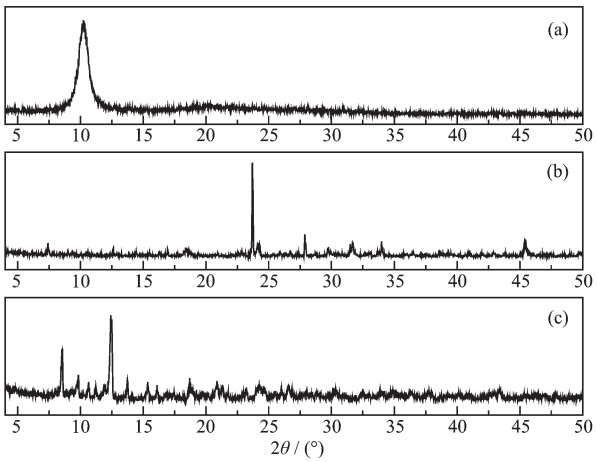

Fig.3　XRD patterns of GOSs (a), (Sm-Gd)BA_3Phen (b) and GOSs/(Sm-Gd)BA_3Phen (c)

2.3　SEM characterization

In order to study the specific morphology of the materials, the SEM images of GOSs, (Sm-Gd)BA_3Phen complex and GOSs/(Sm-Gd)BA_3Phen complex hybrid were obtained. There were many overlapping sheet structures textures in the layer structure in Fig.4 (a),

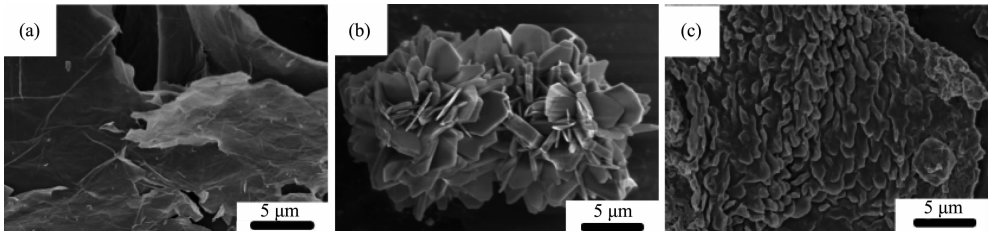

Fig.4 SEM images of GOSs (a), (Sm-Gd)BA_3Phen (b), GOSs/(Sm-Gd)BA_3Phen (c)

which were graphene oxide sheet structure, because they are self-fold and rolling up making GOSs keep a steady state[33]. As can be seen in Fig.4(b), (Sm-Gd)BA_3Phen complex was irregular sheet structure and closely packed together like a flower-like structure. Many seaweed shape structures were adsorbed on the surface of the GOSs in Fig.4(c). After the combination with the graphene oxide, some changes were observed in the morphology of RE complexes. (Sm-Gd)BA_3Phen complex dispersed in the lamellar structure of GOSs, which showed that the (Sm-Gd)BA_3Phen complex coated in the graphene oxide layer structure. The boundaries, curls and wrinkles of GOSs were clearly observed. However, the distribution of (Sm-Gd)BA_3Phen was not uniform because oxygen-containing groups of GOSs were scattered and irregular[22]. In addition, the structure of the seaweed shape could illustrate the reduction of π-π stacking and oxygen-containing groups of GOSs.

2.4 TGA

Fig.5 Shows the thermogravimetric analysis measurements of GOSs, (Sm-Gd)BA_3Phen complex and GOSs/(Sm-Gd)BA_3Phen complex hybrid. TGA was carried out under nitrogen atmosphere with a heating rate of 10 ℃·min^{-1}, and the temperature interval was 20~800 ℃ in the TGA curves. The first stage of GOSs had a weight loss process under 137 ℃, which is due to evaporation of water, corresponding to about 17% in Fig.5(a). The second stage of weight loss was in the temperature interval of 137~289 ℃, corresponding to a weight loss of about 37%, which could be attributed to decomposition of oxygen functional groups[34]. The curve of (Sm-Gd)BA_3Phen complex shows decomposition stages in 300~600 ℃, which could be attributed to the decomposition of (Sm-Gd)BA_3Phen complex. And the process of weight loss under 200 ℃ was due to the evaporation of adsorbed water molecules from the surface of the complex. The weight loss below 268 ℃ of GOSs/(Sm-Gd)BA_3Phen complex hybrid was due to the loss of water and decomposition of oxygen functional groups, correspon-ding to a weight loss of about 2.2%. The second stage of weight loss was between 260 and 487 ℃, corresponding to a weight loss of about 22.2%, which could be attributed to the decomposition of (Sm-Gd)BA_3Phen complex. The third stage of weight loss occured from 487 to 600 ℃, corresponding to a weight loss of about 31.4%, which is due to the loss of GOSs[35]. The DTG curves

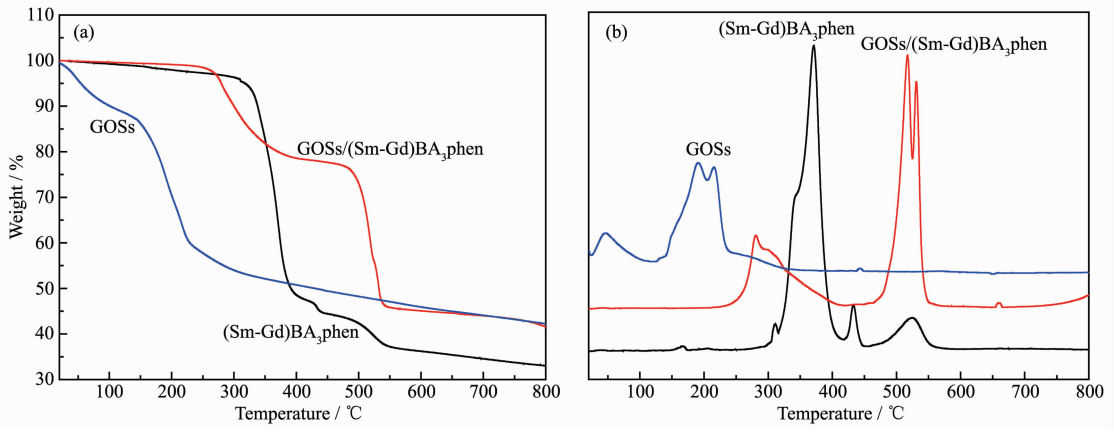

Fig.5 TGA curves (a) and DTG curves (b) of GOSs, (Sm-Gd)BA_3Phen and GOSs/(Sm-Gd)BA_3Phen

(derivative thermogravimetry) of (Sm-Gd)BA_3Phen complex in Fig.5(b) had main mass loss peaks. The peak appeared at 372 ℃, which was different from the GOSs/(Sm-Gd)BA_3Phen at 516 ℃. The results illustrate that the protective effect of oxygen groups in GOSs could improve the decomposition temperature of GOSs/(Sm-Gd)BA_3Phen. We could conclude that the GOSs/(Sm-Gd)BA_3Phen complex hybrid has good thermal stability.

2.5 Fluorescence characterization

Fig.6 shows the digital images of (Sm-Gd)BA_3Phen complex and GOSs/(Sm-Gd)BA_3Phen complex hybrid under daylight and 365 nm UV light. As we can see from Fig.6(b), under daylight, the color of hybrid materials was gray after reacting with GOSs. In addition, the (Sm-Gd)BA_3Phen complex and GOSs/(Sm-Gd)BA_3Phen complex hybrid could present bright red emissions under UV light irradiation under 365 nm UV light. The fluorescence of complex hybrid was stronger than (Sm-Gd)BA_3Phen complex. The results illustrate that GOSs and RE complex are bound together by non-covalent bonds and improve the fluorescence properties of the complex[22].

Luminescence emission and excitation spectra of (Sm-Gd)BA_3Phen complex and GOSs/(Sm-Gd)BA_3Phen complex hybrid have been showed in Fig.7. In the excitation spectra of (Sm-Gd)BA_3Phen complex and GOSs/(Sm-Gd)BA_3Phen complex hybrid, the bands from 310 to 400 nm was related to the $\pi \rightarrow \pi$ transition based on the conjugated double bands of two ligands. The maximum absorption peak was 352 nm. The two spectra are similar, and the fluorescence intensity of GOSs/(Sm-Gd)BA_3Phen complex hybrid was stronger than that of (Sm-Gd)BA_3Phen complex. The result illustrates the presence of GOSs obviously improved the excitation intensity of the complex hybrid.

The emission spectrum of (Sm-Gd)BA_3Phen complex was obtained under excitation at 352 nm. In the emission spectrum, there were three characteristic fluorescence emission peaks, related to 4*f* orbital electronic transitions of $^4G_{5/2} \rightarrow {}^6H_{5/2}$ (563 nm), $^4G_{5/2} \rightarrow$

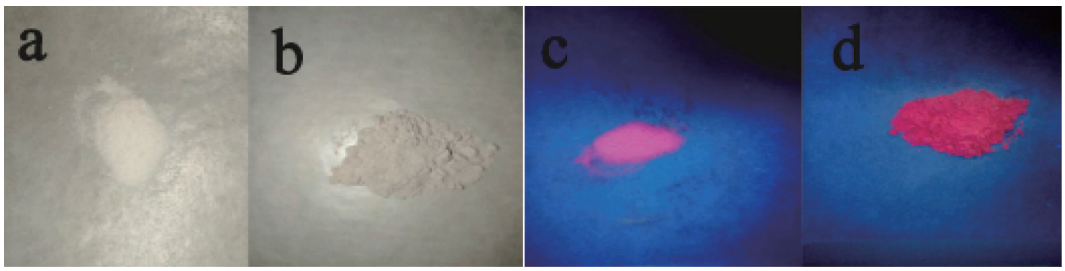

Fig.6 Digital images: (Sm-Gd)BA_3Phen under daylight (a) and under 365 nm UV light (c); GOSs/(Sm-Gd)BA_3Phen under daylight (b) and under 365 nm UV light (d)

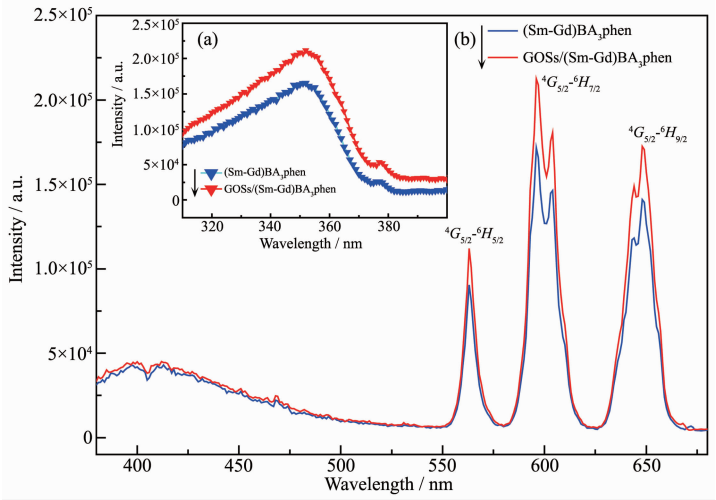

Fig.7 Excitation (a) and emission (b) spectra of (Sm-Gd)BA_3Phen, GOSs/(Sm-Gd)BA_3Phen

$^6H_{7/2}$ (596, 604 nm), $^4G_{5/2}\rightarrow{}^6H_{9/2}$ (643 nm), which are the characteristic peaks of Sm^{3+}[36]. It is well known that Gd^{3+} ions did not have characteristic emission peaks owing to its stable structure ($4f^7$)[14]. Moreover, hybrid materials had bright red luminescence. The strongest fluorescence emission peak corresponds to the $^4G_{5/2}\rightarrow{}^6H_{7/2}$ electron transition at 596 nm. According to the description in the introduction, GOSs had a strong quenching effect. However, the luminescence intensity of GOSs/(Sm-Gd)BA_3Phen complex hybrid was higher than (Sm-Gd)BA_3Phen complex. It could intimate that GOSs do not quench the luminescence of (Sm-Gd)BA_3Phen complex that attached on their surface. It may be due to the unique properties of RE ions that trivalent lanthanide ions have photoluminescence properties. Since the 4*f* valence shells of the trivalent lanthanides were well shielded by the peripheral 5*s* and 5*p* ones, they had preventive effect on external potential quenchers[37-38].

The emission spectra of GOSs/(Sm-Gd)BA_3Phen complex hybrid with different Gd^{3+} or Sm^{3+} molar ratios under excitation 352 nm has been showed in Fig.8. Table 1 shows the result of the excitation and emission intensity, where I_x is the measured fluorescence excitation intensity and I_m is the measured fluorescence emission intensity of complex hybrid. In order to further study the relationship between fluorescent intensity and the concentration of Gd^{3+}, more analyses were carried out. As we can see in Fig.8, all the emission spectra were similar and had the characteristic peaks of Sm^{3+}. Fig.8(b) shows the different Gd^{3+} molar fractions under the wavelength of 596 nm. It could also be seen from the Table 1 that when the amount of Gd^{3+} or Sm^{3+} reached the maximum, the fluorescence intensity of the hybrid was the weakest. The most suitable conditions was obtained through different molar ratios. The intensity reached maximum when $n_{Sm^{3+}}$:$n_{Gd^{3+}}$ was 5:5. It may be due to the energy

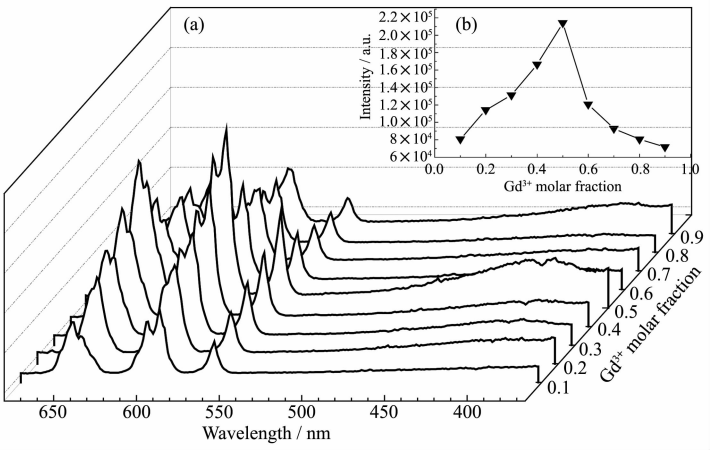

Fig.8 Emission spectra (a) and curves (b) of GOSs/(Sm-Gd)BA_3Phen complexes with different Gd^{3+} molar fractions

Table 1 Fluorescence intensity of GOSs/(Sm-Gd)BA_3Phen

Complex hybrid	$n_{Sm^{3+}}$:$n_{Gd^{3+}}$	Gd^{3+} molar fraction / %	I_x (λ_{ex}=352 nm) / a.u.	I_m (λ_{ex}=596 nm) / a.u.
GOSs/(Sm-Gd)BA_3Phen	1:9	0.9	80 235	71 893
	2:8	0.8	81 245	80 488
	3:7	0.7	102 272	93 030
	4:6	0.6	123 926	120 720
	5:5	0.5	209 639	213 926
	6:4	0.4	165 909	166 477
	7:3	0.3	134 680	131 144
	8:2	0.2	117 445	114 394
	9:1	0.1	82 777	80 741

transfer from Gd^{3+} to Sm^{3+} enhancing the fluorescence performance of the complex hybrids, but excess Gd^{3+} or Sm^{3+} will quench the fluorescence performance.

In order to study the influence of the addition of inert RE element Gd^{3+} on RE complexes, the emission spectrum of (Sm)BA_3Phen and (Sm-Gd)BA_3Phen complexes with $n_{Sm^{3+}}$:$n_{Gd^{3+}}$ being 5:5 under 352 nm excitation have been obtained (Fig.9). The two emission spectra were similar and had the maximum emission peak at 596 nm. Comparing the emission intensity of the two compounds, the fluorescence intensity of RE complexes added with Gd^{3+} was significantly higher. The result illustrates that Gd^{3+} ions play a significant role in improving the luminescence intensity.

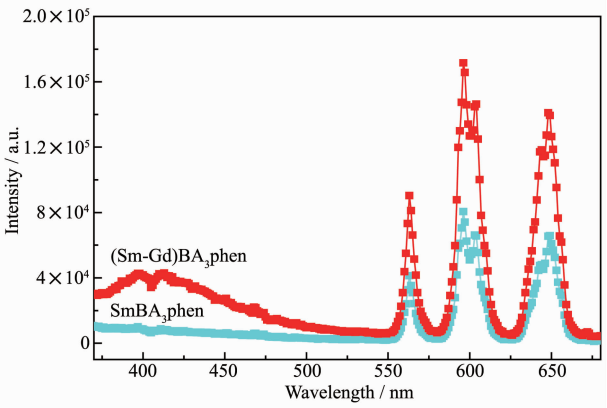

Fig.9　Emission spectra of (Sm)BA_3Phen and (Sm-Gd)BA_3Phen

2.6　Decay lifetime

In order to further understand the properties of material, the study of decay lifetime is also very meaningful. The luminescent lifetime decay curves of (Sm-Gd)BA_3Phen and GOSs/(Sm-Gd)BA_3Phen are shown in Fig.10. In Fig.10, there are two luminescent lifetime decay, the lifetime of (Sm-Gd)BA_3Phen were 0.80 and 63.52 μs, and the lifetime of GOSs/(Sm-Gd)BA_3Phen were 2.19 and 77.64 μs. The luminescent lifetime of GOSs/(Sm-Gd)BA_3Phen was longer than (Sm-Gd)BA_3Phen, which could demonstrate that the complex was deposited on the surface of GOSs. Due to the honeycomb crystal structure of GOSs which limited the rotation and vibration of the RE complex to some extent, the non-radiative transition is reduced to prolong the fluorescence lifetime of the material[19].

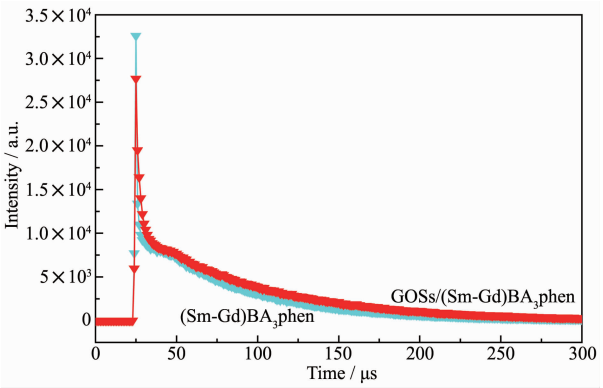

Fig.10　Luminescence decay curves of (Sm-Gd)BA_3Phen and GOSs/(Sm-Gd)BA_3Phen

3　Conclusions

In conclusion, we successfully synthesized a novel heteronuclear RE complex GOSs/(Sm-Gd)BA_3Phen hybrid through non-covalent approach. All products show the characteristic emission peaks of Sm^{3+}. The hybrid materials exhibited strong luminescence intensity, long lifetime and good thermal stability. When $n_{Sm^{3+}}$:$n_{Gd^{3+}}$ was 5:5, the fluorescence intensity was strongest, due to the intramolecular energy transfer. The result proved the existence of GOSs does not quench the luminescence of the Sm^{3+} complex. The great property of the hybrid could be used in many fields and provides an important basis for potential applications such as drug carriers and biomarkers.

Acknowledgments: Thanks to the National Natural Science Foundation Youth Project (Grant No.21701106) and the experimental conditions provided by Shaanxi University of Science and Technology.

References:

[1] Novoselov K S, Geim A K, Morozov S V, et al. *Science*, **2004**,**306**(5696):666-669

[2] Bak S, Kim D, Lee H. *Curr. Appl Phys.*, **2016**,**16**(9):1192-1201

[3] Llobet E. *Sens. Actuators B*, **2013**,**179**:32-45

[4] Liu S L, Liu C, Guo J, et al. *J. Electrochem. Soc.*, **2017**,**164**(12):A2390-A2397

[5] Khurana G, Misra P, Katiyar R S. *Carbon*, **2014**,**76**(9):341-347

[6] Falkovsky L A, Pershoguba S S. *Phys. Rev. B: Condens. Matter*, **2007**,**76**(15):153410
[7] Eda G, Lin Y Y, Mattevi C, et al. *Adv. Mater.*, **2010**,**22**(4):505-509
[8] Xu Y X, Shi G Q. *J. Mater. Chem.*, **2011**,**21**(10):3311-3323
[9] Radovic L R, Mora-Vilches C V, Salgado-Casanova A J A, et al. *Carbon*, **2018**,**130**:340-349
[10]Sun Y, Thiel C W, Cone R L, et al. *J. Lumin.*, **2002**,**98**(1/2/3/4):281-287
[11]Liu S L, He X D, Zhu J P, et al. *Sci. Rep.*, **2016**,**6**:35189
[12]LI Yun-Tao(李运涛), HAI Xiao(海啸), LIU Xia(刘侠), et al. *Chinese J. Inorg. Chem.*(无机化学学报), **2013**,**29**(11):2475-2479
[13]Wani J A, Dhoble N S, Kokode N S, et al. *Luminescence*, **2017**,**32**(2):240-252
[14]Chen Y, Cai W M. *Spectrochim. Acta Part A*, **2005**,**62**(4/5):863-868
[15]Galleani G, Santagneli S H, Ledemi Y, et al. *J. Phys. Chem. C*, **2018**,**122**(4):2275-2284
[16]Kim J, Cote L J, Kim F, et al. *J. Am. Chem. Soc.*, **2010**,**132**(1):260-267
[17]Cao Y W, Yang T, Feng J C, et al. *Carbon*, **2011**,**49**(4):1502-1504
[18]Zou X F, Zhang W J. *RSC Adv.*, **2015**,**5**(68):55143-55149
[19]Wang S J, Hu J B, Wang Y Y, et al. *J. Mater. Sci.*, **2013**,**48**(2):805-811
[20]Fan X Z, Shang K, Sun B, et al. *J. Mater. Sci.*, **2014**,**49**(6):2672-2679
[21]Zhao Y C, Huang L J, Wang Y X, et al. *J. Alloys Compd.*, **2016**,**687**:95-103
[22]Zhang X X, Zhang W J, Li Y J, et al. *Dyes Pigm.*, **2017**,**140**:150-156
[23]Jr W S H, Offeman R E. *J. Am. Chem. Soc.*, **1958**,**80**(6):1339
[24]Wang G C, Yang Z Y, Li X W, et al. *Carbon*, **2005**,**43**(12):2564-2570
[25]Ma Q L, Yu W S, Dong X T, et al. *Opt. Mater.*, **2013**,**35**(3):526-530
[26]Teotonio E E S, Felinto M C F C, Brito H F, et al. *Inorg. Chim. Acta*, **2004**,**357**(2):451-460
[27]Shirvani-Arani S, Ahmadi S J, Bahrami-Samani A, et al. *Anal. Chim. Acta*, **2008**,**623**(1):82-88
[28]Feng H B, Cheng R, Zhao X, et al. *Nat. Commun.*, **2013**,**4**(2):1539
[29]Lerf A, Buchsteiner A, Pieper J, et al. *J. Phys. Chem. Solids*, **2006**,**67**(5/6):1106-1110
[30]Deng R P, Yu J B, Zhang H J, et al. *Chem. Phys. Lett.*, **2007**,**443**(4/5/6):258-263
[31]Fornes T D, Paul D R. *Polymer*, **2003**,**44**(14):3945-3961
[32]Cai D, Song M. *J. Mater. Chem.*, **2007**,**17**(35):3678-3680
[33]Yang D, Velamakanni A, Bozoklu G, et al. *Carbon*, **2009**,**47**(1):145-152
[34]Shen J F, Li T, Shi M, et al. *Mater. Sci. Eng. C*, **2012**,**32**(7):2042-2047
[35]Fan X B, Peng W C, Li Y, et al. *Adv. Mater.*, **2008**,**20**(23):4490-4493
[36]Xia Z G, Chen D M. *J. Am. Ceram. Soc.*, **2010**,**93**(5):1397-1401
[37]Decadt R, Van H K, Depla D, et al. *Inorg. Chem.*, **2012**,**51**(21):11623-11634
[38]Accorsi G, Armaroli N, Parisini A, et al. *Adv. Funct. Mater.*, **2010**,**17**(15):2975-2982